ELSEVIER

Phase synchronization in two coupled chaotic neurons

Jian-Wei Shuai [*], Dominique M. Durand

Department of Biomedical Engineering, Case Western Reserve University, Cleveland, Ohio 44106, USA

Abstract

Chaotically-spiking dynamics of Hindmarsh–Rose neurons are discussed based on a flexible definition of phase for chaotic flow. The phase synchronization of two coupled chaotic neurons is in fact the spike synchronization. As a multiple time-scale model, the coupled HR neurons have quite different behaviors from the Rössler oscillators only having single time-scale mechanism. Using such a multiple time-scale model, the phase function can detect synchronization dynamics that cannot be distinguished by cross-correlation. Moreover, simulation results show that the Lyapunov exponents cannot be used as a definite criterion for the occurrence of chaotic phase synchronization for such a system. Evaluation of the phase function shows its utility in analyzing nonlinear neural systems. © 1999 Published by Elsevier Science B.V. All rights reserved.

1. Introduction

Cooperative behavior is a major focus of study in neuronal systems. The selective synchronization of neural activity has been suggested as a mechanism for binding spatially distributed features into a coherent object [1–3] and too much synchrony may cause dynamical diseases, such as in epilepsy [4,5]. For a periodic neuronal system with the concept of phase, different aspects of coherence, such as phase synchronization, phase-locking, frequency-locking behaviors have been discussed in detail [6]. For coupled chaotic neuronal oscillators, synchronization behavior is detected with the cross-correlation function

[1–3]. Recently, the concept of phase, as well as phase synchronization, has been generalized to the study of chaotic oscillators [7–12]. Phase synchronization has been observed in nonlinear neural, cardiac and ecological systems [13–17]. The oscillations between respiratory and cardiac rhythms [14] or between brain activity and the signals from the flexor muscle [15] show the behavior of phase synchronization. The subthreshold chaotic oscillation of electrically-coupled inferior olivary neurons *in vitro* has also been studied in the view of phase synchronization [16]. Phase synchronization may play an important role in revealing communication pathways in brain [18].

Due to the potential application of phase synchronization in the brain, it is important to study the characteristics of phase dynamics in the neural sys-

---
[*] Corresponding author. Tel.: + 216 368 8534; fax: 216 368 4872; e-mail: jxs131@po.cwru.edu

tem in detail. A flexible definition of phase is presented in Section 2 to analyze the phase of a Hindmarsh–Rose (HR) neuron model [19]. Numerical simulation shows that the interspike interval histogram (ISIH) of the chaotic spikes can be approximately obtained using phase analysis. The simplest synchronizing system is two coupled neurons. Although the synchronization behavior in such a system has been discussed widely [6,20–22], its chaotic dynamics are reconsidered in Section 3 of this Letter in view of phase synchronization. Here we only consider 1:1 phase synchronization [7]. Phase synchronization was first discussed for coupled Rössler oscillators [7–9]. It should be noticed that the dynamics of HR neuron are multiple time-scales [23]. In particular, a fast mechanism is related to the spike process and a slow mechanism is related to the burst process. The Rössler oscillator has only a single time-scale mechanism. Due to this difference, the coupled HR neurons exhibit different synchronizing behaviors from the Rössler oscillators. For coupled Rössler oscillators, the occurrence of phase synchronization corresponds to a decrease in the number of positive Lyapunov exponents [7,9]. However, our simulation shows that Lyapunov exponents in general cannot be used as a criterion for phase synchronization. With the increase of coupling, the synchronization transition in coupled HR neurons goes from burst synchronization to phase synchronization and then toward full synchronization. Synchronization in nonlinear systems is traditionally discussed with cross-correlation [1–3]. To discuss synchronization behavior with phase analysis or cross-correlation, a basic problem which has heretofore been seldom discussed is to determine what different synchronization states they can detect. In Section 4, we show that the phase function can provide a different means to classify synchronization state and detect behaviors that cannot be distinguished by cross-correlation. It also provides different information from other forms of chaotic analysis [24].

2. Phase of chaotic neuron

The phase of a chaotic trajectory can be defined with the Hilbert transform [7]. With such a definition, the phase is globally determined by the whole time series of the signal, rather than the state at a certain point. To give a local definition, the phase can be defined as the angle between the projection of the phase point on the plane and a given direction on the plane [8–11]. The phase can also be defined in the tangent space of the chaotic trajectory [12]. Here, a flexible local definition of phase is proposed. In the chaotic system $\dot{x} = F(x)$ for two variables of interest $s_1(t)$ and $s_2(t)$, which are arbitrary combinations of the state x, i.e., $s_1(t) = s_1(x,\dot{x},\ddot{x},\cdots)$ and $s_2(t) = s_2(x,\dot{x},\ddot{x},\cdots)$, suppose that the attractor in s_1–s_2 plane has only one rotation center. The phase of the system can be defined as:

$$\phi(t) = \arctan \frac{s_1(t) - s_{1c}}{s_2(t) - s_{2c}}. \tag{1}$$

where the point (s_{1c}, s_{2c}) is within the rotation center. Phases defined in Refs. [8–12] are the special cases of Eq. (1). If the rotation is around the origin, the point (s_{1c}, s_{2c}) is often selected to be $(0,0)$ [8,9]. The phase $\phi(t)$ is defined on the whole real line, rather than on the circle $[-\pi, \pi]$ [7]. Because in a typical neural experiment the only observable signal is the membrane action potential $V(t)$, the signals s_1 and s_2 must be generated from $V(t)$. Therefore, a simple possible phase definition can be presented in the planes of $V(t)$–$V(t-\tau)$ [16], $\dot{V}(t)$–$\dot{V}(t-\tau)$, $V(t)$–$\dot{V}(t)$, or $\dot{V}(t)$–$\ddot{V}(t)$. For the first two cases, the time-delay reconstruction is required. The definition of phase in Eq. (1) is flexible because, for a complex system, it permits us to choose a suitable candidate plane in which the attractor has a single rotation center.

Now consider a HR neuron model [19] which is given in Eq. (2) with three variables (x,y,z) and coupling $\varepsilon = 0$.

$$\dot{x}_1 = y_1 - ax_1^3 + bx_1^2 - z_1 + I - \varepsilon(x_1 - x_2),$$

$$\dot{y}_1 = c - dx_1^2 - y_1,$$

$$\dot{z}_1 = r[S(x_1 + \chi_1) + z_1]. \tag{2}$$

$$\dot{x}_2 = y_2 - ax_2^3 + bx_2^2 - z_2 + I - \varepsilon(x_2 - x_1),$$

$$\dot{y}_2 = c - dx_2^2 - y_2,$$

$$\dot{z}_2 = r[S(x_2 + \chi_2) + z_2]. \tag{3}$$

The HR neuron is widely investigated as a simple model of nonlinear neurons [22,25]. Each neuron is characterized by three time-dependent variables: the membrane potential x, the recovery variable y, and a slow adaptation current z. The external input is given by I. In the simulation, let $a = 1.0$, $b = 3.0$, $c = 1.0$, $d = 5.0$, $s = 4.0$, $r = 0.006$, $\chi = 1.56$ and $I = 3.0$. Because the HR neuronal model has multiple time-scale dynamics [23], the burst of action potentials often consists of a group of spikes on a slow depolarizing wave. Numerical simulation shows that the neuron is chaotic with maximum Lyapunov exponent 0.01. Unlike the Lorenz oscillator with two rotation centers [10,11], the trajectory in the x–z plane, as shown in Fig. 1(a), consists of infinite rotation centers. The attractors in different planes containing x are given in Fig. 1(b–d). It can be seen that the attractor has a single rotation center in the $x(t)$–$x(t-\tau)$, $\dot{x}(t)$–$\dot{x}(t-\tau)$ and the $\dot{x}(t)$–$\ddot{x}(t)$ plane. The attractor in the $x(t)$–$x(t-\tau)$ plane has a tail due to the slow depolarizing wave. The phases of the chaotic attractor in these planes are given in Fig. 2(a) with time from 0 to 300. The corresponding membrane potential of the neuron is given in
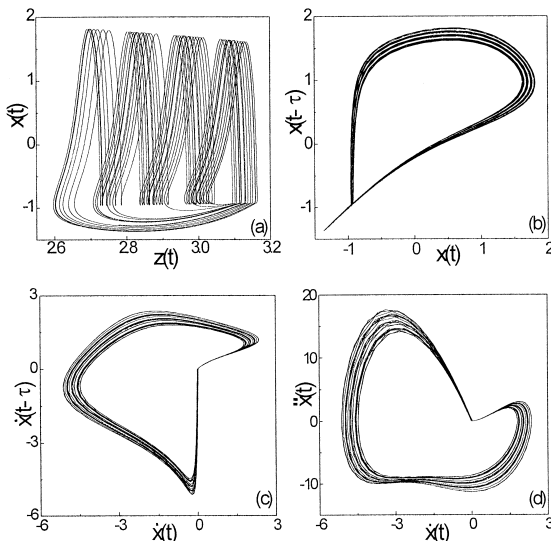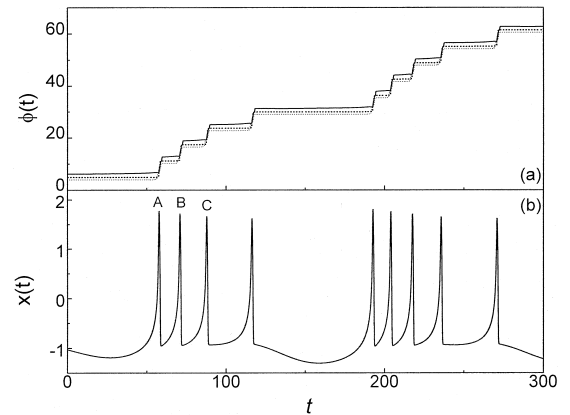

Fig. 2. Three phases of the chaotic HR neuron in different planes versus time from 0 to 300 (a) and its corresponding chaotic spiking trajectory (b). In (a), the upper solid line is calculated with $\phi(t) = \arctan[\dot{x}(t-\tau)/(\dot{x}(t)+0.1)]$, the middle dashed line is with $\phi(t) = \arctan x(t-\tau)/x(t)$, and the lower dotted line is with $\phi(t) = \arctan[(\ddot{x}(t)+5.0)/(\dot{x}(t)+1.0)]$.

Fig. 1. Attractor of a HR neuron in the z–x plane (a), the $x(t)$–$x(t-\tau)$ plane (b), the $\dot{x}(t)$–$\dot{x}(t-\tau)$ plane (c), and the $\dot{x}(t)$–$\ddot{x}(t)$ plane (d). In the Letter, the time delay $\tau = 0.5$ is used.

Fig. 2(b). Except for the initial phases, these three definitions of phase lead to nearly identical results. The phase of neuron changes fast when the neuron spikes; otherwise, the phase changes slowly. When a spike occurs, the phase increases by a value of 2π.

It is known that neuronal information is mainly transmitted using a code based on the time intervals between neuronal firings rather than the spiking amplitude [26]. Thus, an important concept in sensory information is the ISIH, which is calculated from the successive spiking peaks of the membrane potential. Using the phase variable, one can define a time interval between phases with 2π-jump. Unlike ISIH, 2π-phase interval is not directly related to the amplitude of the action potential. For a periodic trajectory the two definitions of time intervals give the same results, while for a chaotic trajectory they cannot give the exactly same results. For example, the phase differences between successive spikes of A and B, or B and C in Fig. 3 are 6.31 and 6.24, respectively, which differ slightly from 2π with the error 0.7%. However, Fig. 3 show that the ISIH and the 2π-phase interval histogram (2π-PIH) both give a similar distribution in the interval histogram. The similarity between ISIH and 2π-PIH suggests that the interval
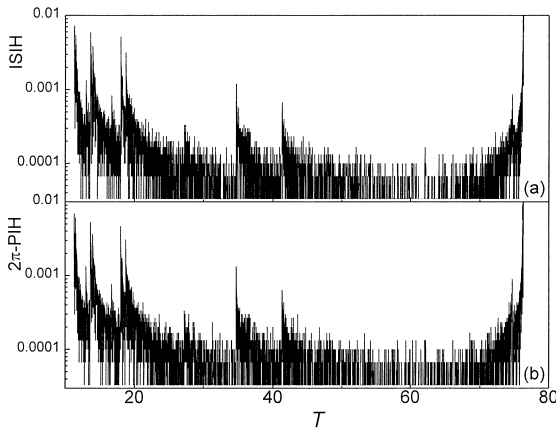
Fig. 3. Interspike interval histogram (ISIH) (a) and the 2π-phase interval histogram (2π-PIH) (b) of the chaotic HR neuron.

histogram of the chaotic dynamics can be discussed with the continuous variable of phase.

3. Phase synchronization of two coupled neurons

To examine phase synchronization, we modulate the excitable coupling parameter ε in Eq. (2) and Eq. (3). Phase synchronization occurs when the phases of two oscillators have the continual relationship $\phi_1(t) \approx \phi_2(t)$ with time [7,8]. As discussed above, only when a spike occurs, the phase increases by a value of 2π. Thus phase synchronization means that the two neurons always generate spikes almost simultaneously. So phase synchronization is spike synchronization. This result agrees with the definition of phase synchronization in periodic neuronal systems [6]. With the knowledge of phase $\phi(t)$, the frequency $\omega(t) = \dot{\phi}(t)$ and the mean frequency $\Omega = \langle \dot{\phi} \rangle = \lim_{T \to \infty}(\phi(T) - \phi(0))/T$ can be defined [8]. Thus, for the coupled systems, weak phase synchronization, i.e., frequency-locking state for $\Delta\Omega = \Omega_1 - \Omega_2 \to 0$, is defined [8]. Frequency-locking behavior means that the two coupled neurons have the same average spiking frequency.

Suppose the two neurons discussed here are slightly different with $\chi_1 = 1.56$ and $\chi_2 = 1.57$ respectively. Simulation results show that when the coupling $0 \leq \varepsilon \leq 0.1$ or $\varepsilon \geq 0.3$, an attractor with a single rotation center can be observed in the $\dot{x}(t)$–$\dot{x}(t - \tau)$ or $\dot{x}(t)$–$\ddot{x}(t)$ plane and thus the phase can

be defined for both neurons. In the following simulation, we only discuss the phase of the attractor in the $\dot{x}(t)$–$\dot{x}(t - \tau)$ plane with time delay $\tau = 0.5$ and the center point $(-0.1, 0)$. Without coupling, the mean frequencies of two neurons are 0.187 and 0.182, respectively.

Some statistical properties of the two coupled neurons versus the electric coupling ε are given in Fig. 4 with $0.3 < \varepsilon < 0.7$. The plot of the difference $\Delta\Omega$ of the mean frequencies versus ε is shown in Fig. 4(a). Fig. 4(b) gives the maximum value
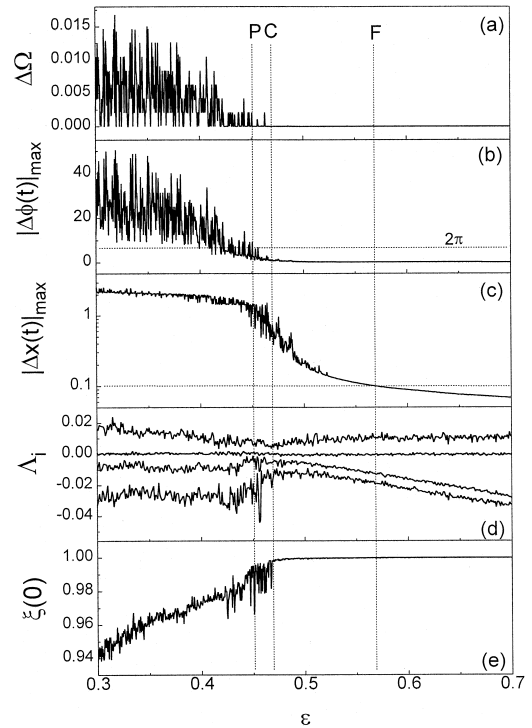

Fig. 4. Some statistical properties of the two coupled model versus the electric coupling ε. (a) The difference of the mean frequencies between two neurons; (b) The maximum absolute difference of two phases. The dotted horizontal line is for the value of 2π. (c) The maximum absolute difference of two potential trajectories. The dotted horizontal line is for the value of 0.1. (d) The four largest Lyapunov exponents of the coupled system ; and (e) the cross-correlation $\xi(0)$ at $\tau = 0$. The dotted vertical line P is for $\varepsilon = 0.45$, i.e., the transition point of phase synchronization; the dotted vertical line C is for $\varepsilon = 0.47$, i.e., the transition point of cross-correlation; the vertical line F is for $\varepsilon = 0.57$, i.e., the transition point of nearly full synchronization. The simulation results are obtained with time from 1000 to 4000 after the transient process of time from 0 to 1000.

$|\Delta\phi(t)|_{max}$ of the absolute phase difference $|\phi_1(t) - \phi_2(t)|$. Simulation results show that $\Delta\Omega < 0.0001$ and $|\Delta\phi(t)|_{max} < 2\pi$ occur typically in the region of $\varepsilon > 0.45$. The relation of $|\Delta\phi|_{max} < 2\pi$ means that, when there is a spike in one neuron, a corresponding spike is being instantaneously excited in the other neuron. Thus, the phases of two neurons are synchronizing in the region of $\varepsilon > 0.45$. The maximum value $|\Delta x(t)|_{max}$ is plotted in Fig. 4(c). Due to the slight differences in the two neurons, their trajectories cannot be identical no matter what value the coupling is. However, Fig. 4(c) shows that in the region of $\varepsilon > 0.57$ the value of $|\Delta x|_{max}$ is typically smaller than 0.1. Here the value 0.1 is quite smaller than the typical scale of the HR neuron attractor that is about 3.6. Therefore, Fig. 4(c) suggests that the amplitudes of two neuron potentials are strongly correlated in the region of $\varepsilon > 0.57$ and so the two coupled neurons in such a region are here termed as nearly full synchronization. In the region of $0.45 < \varepsilon < 0.57$, the two neurons are typically characterized as phase synchronization, meaning that the phases of two neurons are strongly correlated but the amplitudes of their potentials are weakly correlated.

An intermittent behavior between frequency-locking and non-frequency-locking is typically found in parameter space for $0.3 < \varepsilon < 0.45$. Such an intermittence is also found for $0 < \varepsilon < 0.1$. It has been shown that the frequency-locking behavior for Rössler or Lorenz systems is related to a decrease of the number of positive Lyapunov exponents [7,9,12]. Unlike those systems, our simulation shows that there is not such a relationship for coupled HR oscillators. Without coupling, both oscillators have a positive, a negative and a zero exponent. As the coupling strength increases to 0.08, two zero exponents become negative and one of the positive exponents becomes zero. The plots of the four largest Lyapunov exponents versus ε are calculated in Fig. 4(d) with $0.3 < \varepsilon < 0.7$. In fact, in the region of $\varepsilon > 0.08$, all signs of six Lyapunov exponents of the system remain unchanged: one positive, one zero, and four negative. This observation indicates that Lyapunov exponents in general cannot be used as the definite criterion for frequency-locking synchronization.

Now we discuss four examples in detail with the coupling $\varepsilon = 0.60$, 0.46, 0.353 and 0.35, each as an example of nearly full synchronization, phase synchronization, frequency-locking state and non-frequency-locking state, respectively. Their trajectories in the x_1–x_2 plane are drawn in Fig. 5, which can show the correlativity between potentials of x_1 and x_2. The plots of phase difference $\Delta\phi(t) = \phi_1(t) - \phi_2(t)$ versus time t are given in Fig. 6(a), which show the correlativity between phases of ϕ_1 and ϕ_2. For $\varepsilon = 0.60$, the phases of the two neurons closely approach each other with time and the trajectory in the x_1–x_2 plane is in a small-δ neighborhood of subspace with $\delta = 0.09$. Thus, the two neurons are in nearly full synchronization state. For $\varepsilon = 0.46$, the two phases are also quite close to each other with time, while a little weaker correlation between the amplitudes of potentials x_1 and x_2 can be seen from Fig. 5(b). As a result, it is characterized as phase synchronization. With $\varepsilon = 0.353$, the two neurons are frequency-locked with quite weak amplitude correlation. As shown in Fig. 6(a) with the gray dotted line, at times the phase differences are about zero, at times they are about 2π. For some small time intervals the phase difference can be as large as 4π. These observations mean that at times two coupled neurons generate spikes instantaneously, at times one neuron can spike 1 or 2 more spikes than the other one. So, the frequency-locking state between two
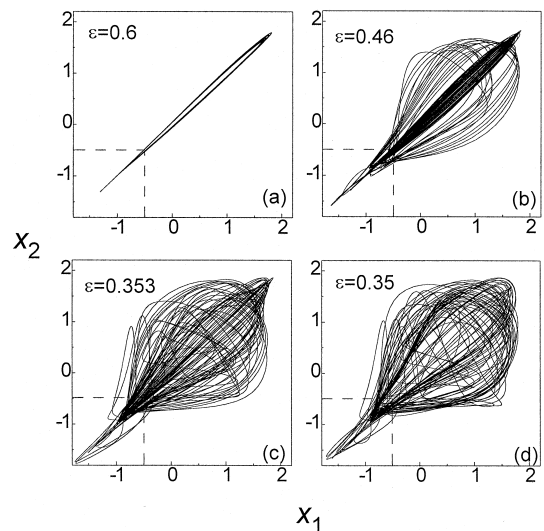

Fig. 5. Potential trajectories of two coupled neurons in the x_1–x_2 plane with (a) $\varepsilon = 0.6$, (b) 0.46, (c) 0.353 and (d) 0.35. The dotted lines are for $x_{1,2} = -0.5$. The state with x_1 or $x_2 > -0.5$ indicates the spike state.
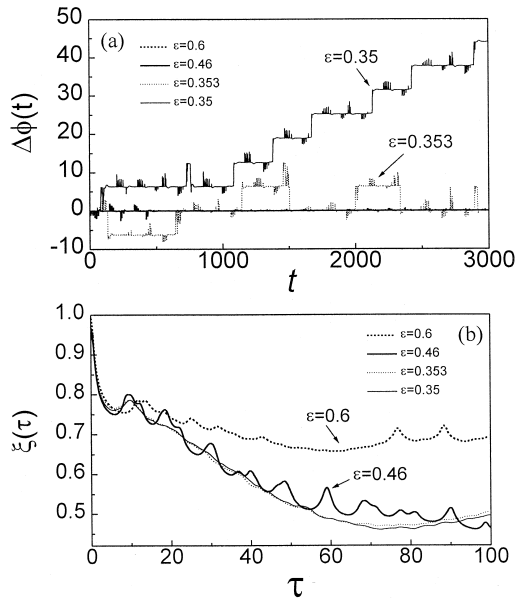
Fig. 6. Plots of (a) the phase difference between two HR neurons versus time t from 0 to 3000 and (b) the cross-correlation of two trajectories versus time shift τ from 0 to 100 with $\varepsilon = 0.6$, 0.46, 0.353 and 0.35. In (a), the absolute phase differences for $\varepsilon = 0.6$ versus ε are always smaller than 0.16. So the curve of $\varepsilon = 0.6$ is typically covered by the curve of $\varepsilon = 0.46$.

coupled neurons can be viewed as an intermittent phase synchronization. A non-frequency-locking example is given with $\varepsilon = 0.35$. Because the mean frequencies of the two neurons are different, their phase difference increases linearly with time, i.e., $\Delta\phi(t) = 1.6 \times 10^{-3}t$, as given in Fig. 6(a) with the gray line. For the couplings of $\varepsilon = 0.353$ and 0.35, Fig. 6(a) shows two typical phase jumps. The first one is the 2π-step of phase difference, meaning that one neuron fires alone. Such a 2π-jump is also observed in coupled Rössler or Lorenz oscillators [11]. The second jump is the $\alpha \cdot 2\pi$-impulse with $\alpha \leq 1.0$, which occurs when one neuron fires first and the other is driven to spike after a short time lag.

4. Phase function and cross-correlation

The cross-correlation function $\xi(t)$

$$\xi(\tau) = \frac{\langle x_1(t) x_2(t+\tau)\rangle}{\left(\langle x_1^2(t)\rangle\langle x_2^2(t)\rangle\right)^{1/2}} \quad (4)$$

versus time shift τ is plotted in Fig. 6(b) for the four examples above. A sharp peak at $\tau = 0$ for $\xi(t)$ is

obtained for each example. In fact, simulation results show that a sharp peak at $\tau = 0$ with $\xi(0) > 0.94$ can be observed for coupled HR neurons with $\varepsilon > 0.3$, as given in Fig. 4(e). So, viewed from the cross-correlation, the coupled neurons are all characterized as synchronization states in the region of $0.3 < \varepsilon < 0.7$. However, it seems that Fig. 5(c & d) strongly suggest that the potentials of two neurons are weakly correlated, rather than synchronization. Here we show that these different observations are original to the multiple time-scale dynamics of HR neuron.

With multiple time-scale dynamics, the HR neuron has a fast mechanism which is related to the spike process and a slow mechanism which is related to the burst process [23]. For two coupled HR neurons, the burst synchronization is first observed. With a stronger coupling, the spike synchronization can occur. Fig. 7(a) gives the trajectories of two neurons with $\varepsilon = 0.35$. For this example, simulation results show that the average time interval of a rest state (typically with $-1.8 < x < -0.9$) is about 85 and the average time interval of a burst state (typically with $-0.9 < x < 1.8$) is about 80. Each burst consists of an average of 8 spikes. For $x > -0.5$, a spike only lasts for a time interval of 4. These values suggest that the trajectory spends most of time (about $1 - (4 \times 8)/(85 + 80) \approx 81\%$) in the region of $-1.8 < x < -0.5$ that is related to the non-spike states.
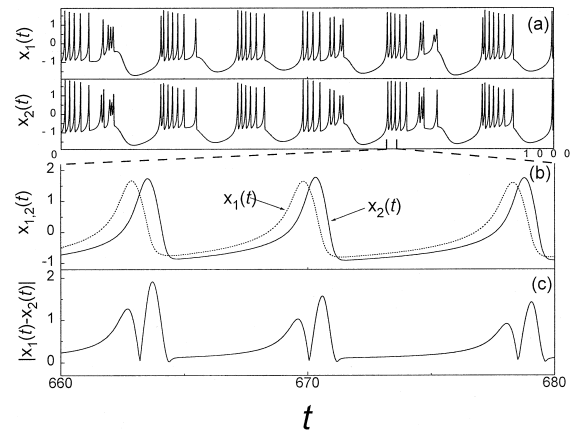

Fig. 7. The trajectories $x_1(t)$ and $x_2(t)$ of two neurons with $\varepsilon = 0.35$. (a) The time interval is from 0 to 1000. (b) A enlarged figure of (a) with time from 660 to 680 and (c) their absolute difference. In figure (b) the time lags between two nearby peaks are all about 0.5.

Thus, once the burst synchronization occurs, the value of $\xi(0)$ will approach to 1. For this example $\xi(0) = 0.96$ is obtained. This discussion shows that, for HR neurons, the cross-correlation primarily captures the burst synchronization. As a result, Fig. 4(e) indicates that the coupled neurons in the region of $0.3 < \varepsilon < 0.7$ are all in burst synchronization.

In burst synchronization state, the trajectories of two neurons in the $x_1 - x_2$ plane should approach the diagonal line $x_1 = x_2$ in the non-spike region $x_1, x_2 < -0.5$. This can be confirmed by Fig. 5. However, Fig. 7(b & c) also shows that, because a spike is very fast, even a short time-lag between two neurons (e.g. 0.5), can induce a large potential difference (e.g. $\Delta x > 2.0$). Thus, large deviations from the diagonal line $x_1 = x_2$ are observed in Fig. 5(b, c & d) in the spike region $x_1, x_2 > -0.5$, because of the weak correlativity of spikes between two neurons.

So, for coupled HR neurons the phase synchronization occurs when cross-correlation is large. As discussed, this is because HR neuron is a multiple time-scale system. Unlike the HR neuron, the Rössler oscillator has a single time-scale mechanism. Simulation results show that for coupled Rössler oscillators phase synchronization occurs when cross-correlation is small. For coupled Rössler oscillators given by Eq. (3) in Ref. [7], a transition between frequency-locking and non-frequency-locking states occurs around the coupling $C \approx 0.028$ [7,12], as given in Fig. 8(a). The cross-correlation $\xi(0)$ between x_1 and x_2 without any time-lag versus the coupling C is calculated in Fig. 8(b). It is shown that $\xi(0) < 0.3$ for $C < 0.03$.

Any similarity between two trajectories can translate to a peak in cross-correlation. The sharp peak at $\tau = 0$ with $\xi(0) > 0.94$ for coupled HR neurons with $\varepsilon > 0.3$ indicates that such a similarity has no time lag. So, lag synchronization [9] does not occur in coupled HR neurons. It has been shown that with the increase of coupling, the synchronization transition in two coupled Rössler oscillators is from phase synchronization to lag synchronization to nearly full synchronization [9]. Our simulation shows that HR neurons follow a different transition route, i.e., from burst synchronization to phase synchronization to nearly full synchronization. Due to the presence of burst synchronization in HR neurons, lag synchronization does not occur in the transition from phase synchronization to nearly full synchronization.
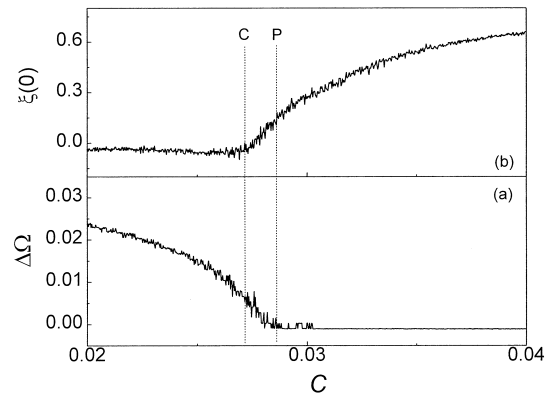

Fig. 8. For coupled Rössler oscillators, (a) the plot of the difference of the mean frequencies versus the coupling C and (b) the cross-correlation $\xi(0)$ between x_1 and x_2 without any time-lag versus the coupling C. The dotted vertical line P is for $C = 0.028$, i.e., the transition point of phase synchronization; the dotted vertical line C is for $\varepsilon = 0.027$, i.e., the transition point of cross-correlation.

Fig. 4(e) shows that there is a transition point at $\varepsilon \approx 0.47$ for cross-correlation. This transition should be related to the occurrence of spike synchronization. But such a transition point is different from the transition point of phase synchronization, i.e. $\varepsilon = 0.45$. Similar, Fig. 8(b) shows that a transition point given by cross-correlation is at $C \approx 0.027$, rather than 0.028. Around $\varepsilon \approx 0.47$ for coupled HR neurons or $C \approx 0.027$ for coupled Rössler oscillators, there is a transition of synchronization, which is detectable by both phase function and cross-correlation. In general, the cross correlation strongly depends on the amplitude of trajectory, while the phase function largely ignores amplitude information. Therefore, they provide different means to classify synchronization states and give different transition results.

From Fig. 6(b), one can also see that the cross-correlation functions for $\varepsilon = 0.35$, 0.353 and 0.45 are quite similar. However, viewed using the phase function, they exhibit quite different behaviors. For coupling HR neurons having burst and spike dynamics, the cross-correlation primarily captures burst synchronization, while the phase function concentrates solely on the spike state. For two burst-synchronized neurons, their spikes can be weakly correlated, have the same average frequency, or be strongly correlated. Thus, for different coupled HR

systems, although their cross-correlations may be indistinguishable, their phase analysis can be quite different.

In Ref. [24] a phenomenon of synchronization of the mean frequencies of switching in coupled chaotic bistable Lorenz oscillators has been discussed. The chaotic Lorenz system is considered a bistable system. Being a bistable system, it is then possible to define the mean frequency of transitions from one state to another and also the mean frequency of switching. The synchronization of the mean frequencies of switching means that with a large coupling the mean frequencies of switching of two Lorenz oscillators can approach each other. For an excitable neuron, two typical state, i.e., a rest state and an exciting state, can be distinguished, and then the synchronization of mean frequencies of switching can be discussed. However, unlike the bistable process, the phase function is typically defined for the attractor that has a single rotation center. For HR neuron, the phase function concentrates solely on the fast spikes, rather than the exciting state which consists of the burst and spike states. So it can be expected that the phase function and mean frequency of switching define the different synchronization states.

5. Conclusions

In summary, the spiking dynamics of chaotic excitable HR neurons as an example of multiple time-scales dynamics are discussed based on a flexible definition of phase for chaotic flow. When a spike occurs, the phase of the neuron increases by a value of 2π. The ISIH of the chaotic neuron can be approximated by the 2π-PIH. For two coupled chaotic HR neurons, the phase synchronization is in fact the spike synchronization. As a multiple time-scale model, the coupled HR neurons have quite different behaviors from the single time-scale Rössler oscillators. We show that for such a coupled system the Lyapunov exponents cannot be used as a definite criterion for the occurrence of frequency-locking synchronization, and with the increase of coupling two slightly different HR neurons evolve from burst synchronization to phase synchronization and finally toward to full synchronization. Compared to the

cross-correlation, the phase function classifies synchronization states by different means. For multiple time-scale HR neurons, cross-correlation primarily captures burst synchronization, while the phase function mainly concentrates on the spike synchronization. Furthermore, the phase function can detect behaviors that cannot be distinguished by cross-correlation. Therefore, our research suggests that the phase function is a useful nonlinear dynamical tool providing information relating to the ISIH and spike synchronization of neural systems.

References

[1] C.M. Gray, P. Lonig, A.K. Engel, W. Singer, Nature 338 (1989) 334.
[2] M.A. Whittington, R.D. Traub, J.G.R. Jefferys, Nature 373 (1995) 612.
[3] J. Sarnthein, H. Petsche, P. Rappelsberger, G.L. Shaw, A. von Stein, Proc. Natl. Acad. Sci. USA 95 (1998) 7092.
[4] C.P. Taylor, F.E. Dudek, Science 218 (1982) 810.
[5] D.M. Durand, E.N. Warman, Journal of Physiology 480 (1994) 527.
[6] R.E. Mirollo, S.H. Strogatz, SIAM J. Appl. Math. 50 (1990) 1645.
[7] M.G. Rosenblum, A.S. Pikovsky, J. Kurths, Phys. Rev. Lett. 76 (1996) 1804.
[8] G.V. Osipov, A.S. Pikovsky, M.G. Rosenblum, J. Kurths, Phys. Rev. E 55 (1997) 2353.
[9] M.G. Rosenblum, A.S. Pikovsky, J. Kurths, Phys. Rev. Lett. 78 (1997) 4193.
[10] A.S. Pikovsky, M.G. Rosenblum, G.V. Osipov, J. Kurths, Physica D 104 (1997) 219.
[11] K.J. Lee, Y. Kwak, T.K. Lim, Phys. Rev. Lett. 81 (1998) 321.
[12] J.Y. Chen, K.W. Wong, J.W. Shuai, (submitted).
[13] D.J.D. Earn, P. Rohani, B.T. Grenfell, Proc. R. Soc. Lond. B 265 (1998) 7.
[14] C. Schader, M.G. Rosenblum, J. Kurths, H. Abel, Nature 392 (1998) 239.

[15] P. Tass, M.G. Rosenblum, J. Weule, J. Kurths, A. Pikovsky, J. Volkmann, A. Schnitzler, H.J. Freund, Phys. Rev. Lett. 81 (1998) 3291.

[16] V. Makarenko, R. Llinas, Proc. Natl. Acad. Sci. USA 95 (1998) 15747.

[17] B. Blasius, A. Huppert, L. Stone, Nature 399 (1999) 354.

[18] R. Fitzgerald, Physics Today March, 17 (1999).

[19] J.L. Hindmarsh, R.M. Rose, Proc. R. Soc. London B 221 (1984) 87.

[20] G. Renversez, Physica D 114 (1998) 147.

[21] D. Terman, N. Kopell, A. Bose, Physica D 117 (1998) 241.

[22] R. Huerta, M.I. Rabinovich, H.D.I. Abarbanel, M. Bazhenov, Phys. Rev. E 55 (1997) R2108.

[23] J. Rinzel, Y.S. Lee, J. Math. Biol. 25 (1987) 653.

[24] V.S. Anishchenko, A.N. Silchenko, I.A. Khovanov, Phys. Rev. E 57 (1998) 316.

[25] W. Wang, G. Chen, Z.D. Wang, Phys. Rev. E 56 (1997) 3728.

[26] J.C. Eccles, The Understanding of the Brain (McGraw-Hill, New York, 1973).